Journal of Structural Geology 45 (2012) 68–86

Contents lists available at SciVerse ScienceDirect

Journal of Structural Geology

journal homepage: www.elsevier.com/locate/jsg

Structure and geological history of the Carboneras Fault Zone, SE Spain: Part of a stretching transform fault system

E.H. Rutter [a,*], D.R. Faulkner [b], R. Burgess [a]

[a] University of Manchester, School of Earth, Atmospheric and Environmental Sciences, Manchester M13 9PL, UK
[b] University of Liverpool, Earth and Ocean Sciences, School of Environmental Sciences, Liverpool L69 3GP, UK

ARTICLE INFO

Article history:
Received 17 November 2011
Received in revised form
17 April 2012
Accepted 1 May 2012
Available online 24 August 2012

Keywords:
Fault zone structure
Carboneras fault
Geological history
Fault gouge
Stretching transform fault
SE Spain

ABSTRACT

The Carboneras Fault Zone (CFZ), is a major NE–SW trending tectonic lineament in SE Spain. Active from upper-Miocene to Recent times, it separates the volcanic Cabo de Gata terrain to the SE (accumulated over 18–6 Ma BP) from the tract of uplifted Alpine metamorphic basement blocks and post-orogenic basins that comprise the Betic Cordilleras lying to the NW. New geological mapping and age determinations have been used to constrain the geometry and geological history of the fault zone.

The CFZ consists of left-lateral strike-slip faults bearing fault gouge formed in the uppermost 5 km of the crust. The faults cut metamorphic basement and folded post-orogenic sediments and volcanic rocks, and acted as a conduit for calc-alkaline volcanic rocks rising to the surface. NW of the CFZ, a series of unconformities and deformation episodes affect successive sedimentary formations of upper Miocene age. The CFZ is interpreted as part of a transform fault system separating NE–SW stretched and NW–SE shortened crust deformed above a south-westward retreating subducted slab, from a less deformed terrain lying to the south-east. Total offset on the CFZ may be up to 40 km but is at least 15 km.

1. Introduction

The left-lateral strike-slip Carboneras Fault Zone (CFZ), in the south-east of the Iberian peninsula, displaces metamorphic basement rocks of the Betic Cordilleras against Miocene calc-alkaline volcanic rocks (Fig. 1) (Rutter et al., 1986; Sanz de Galdeano, 1990; Turner et al., 1999; Scotney et al., 2000). It also affects Miocene and Pliocene rocks of the north-eastern part of the Nijar basin. Its onshore outcrop has also been termed the Serrata fault (e.g. Boorsma, 1992; Huibregtse et al., 1998). Here we shall refer to the entire onshore fault zone as the Carboneras Fault Zone (CFZ). The total displacement across the CFZ is not precisely known, but is locally expected to be more than 15 km, principally to account for the lack of preservation of Miocene volcanic rocks on the NW side of the fault zone where it is not buried beneath Pliocene deposits. A related system of left-lateral strike-slip fault segments also extends further north-east, including the Palomares and Alhama de Murcia faults (Fig. 2), the latter extending almost as far north-east as Alicante.

The NE–SW trending fault zone extends southwards across the Alborán Sea basin (LeBlanc and Olivier, 1984; De Larouzière et al., 1988; Grácia et al., 2006), where it is one of a group of perhaps linked faults that has been termed the trans-Alborán shear zone, extending into north Africa as the Nekor and Jebha faults. The great length of this complex of strike-slip faults (450 km) probably implies that the faulting extends right through the continental crust and into the upper mantle, and by implication might be expected to play an important role in the Neogene geodynamic evolution of the western Mediterranean. Of these fault segments the CFZ is particularly well exposed at its north-eastern end. To understand the geodynamic role of the fault system requires a clear appreciation of its structure and geological history in the Carboneras segment.

Geological maps from previous studies in the north-eastern part of the outcrop of the CFZ cover all or part of this area in varying degrees of detail (e.g. Westra, 1969; Garcia Monzón et al., 1974; Rutter et al., 1986; Van der Poel, 1992; Keller et al., 1995; Huibregtse et al., 1998; Scotney et al., 2000; Fortuin and Krijgsman, 2003; Faulkner et al., 2003). In this paper we report the results of new geological mapping of the exposed part of the CFZ, mainly at a scale of 1:10,000 but sometimes at larger scale. This is augmented with new ^{40}Ar–^{39}Ar dating of rocks of the volcanic sequence. We believe that the present mapping provides the basis for a first coherent

* Corresponding author.
E-mail address: e.rutter@manchester.ac.uk (E.H. Rutter).

0191-8141
http://dx.doi.org/10.1016/j.jsg.2012.08.009

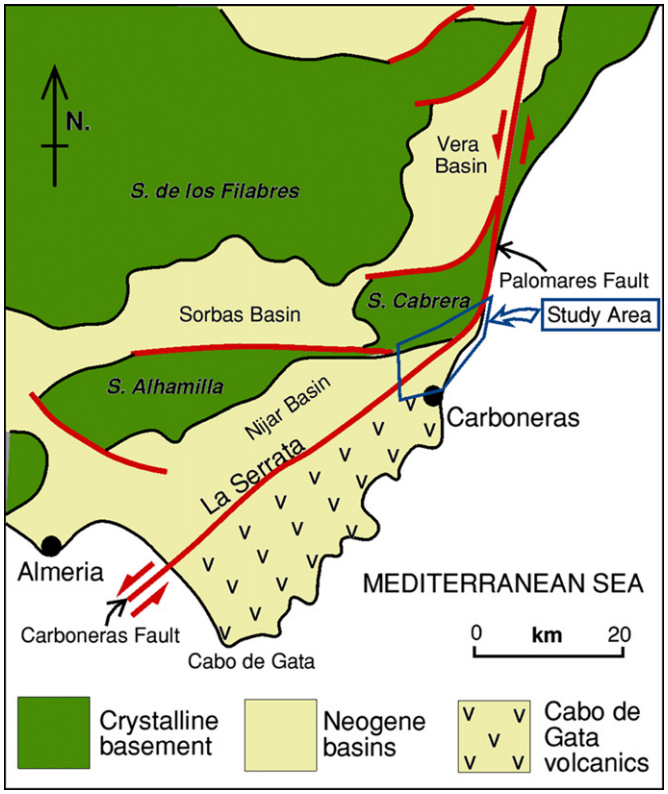

Fig. 1. Outline map of SE Spain showing the disposition of uplifted basement blocks (Sierras) and the Neogene sedimentary basins that are often bounded by major faults. La Serrata is a topographic ridge of intrusive igneous rocks that outcrops for about one-third the length of the onshore outcrop of the Carboneras fault.

interpretation of the geological history of the area and its place in the overall geodynamic scheme.

This study forms part of a collaborative program to investigate the in-situ seismic properties of a large fault zone using high-resolution seismic tomography in a region where the results of the seismic studies can be verified by direct geological observation. We previously reported detailed studies of the structure of the fault rocks of the CFZ (Rutter et al., 1986; Faulkner et al., 2003) and measurements of the permeability to fluids (gas and water) of the fault gouges (Faulkner and Rutter, 2000, 2003). These have now been complemented by laboratory measurements of acoustic wave velocities with forward modelling to account for crack arrays and in order to permit comparison with our in-situ seismic studies. These results will be presented in due course.

The geodynamic framework of which the fault system forms part is set out, followed by a description of structural and stratigraphic relations in the main rock groups of the area. These comprise the basement rocks, the volcanic rocks of the Cabo de Gata series, the post-orogenic sedimentary rocks, and a description of how the area can be divided into lithotectonic blocks bounded by major faults and unconformities, emphasizing the lithostratigraphic differences to the NW and SE of the CFZ. The fault zone itself and its rock products are described, and the observations are collected into an interpretive summary of the temporal and geometric evolution of the area and of its regional tectonic significance.

Grid references of particular localities mentioned in the text and used on Fig. 3 are given in the UTM (Universal Transverse Mercator) coordinate system that is used on the IGN (Instituto Geográfico Nacional) topographic maps, European 1950 datum.

2. Geodynamic framework

The deep-seated deformation and metamorphism of the internal zone of the Betic Cordilleras culminated during early Miocene time (25–20 Ma BP) with rapid tectonic unroofing and cooling of metamorphic basement rocks by extensional collapse of the orogen (Platt and Vissers, 1989; Zeck, 1996; Platt and Whitehouse, 1999; Vissers, 2012). For the subsequent Miocene through Recent evolution of the region, the scheme proposed by Lonergan and White (1997) and further elaborated by Gutscher et al. (2002), Faccenna et al. (2004), Gutscher (2012, 2012) seems best compatible with the present day structure and seismicity, and with studies of the Neogene tectonics of the Betic Cordilleras (e.g. Booth-Rea et al., 2004; Sanz de Galdeano and Alfaro, 2004; Sanz de Galdeano and Buforn, 2005; Martínez-Martínez et al., 2006; Meijninger and Vissers, 2006; Grácia et al., 2006; Giaconia et al., 2011).

Fig. 2 shows in outline the model which is based on NE–SW stretching of the Betic zone crust and underlying lithospheric mantle to the NW of the CFZ as a result of SW-directed rollback of a short segment of steeply descending subducted lithosphere. Its present position is immediately beneath the western Betic-Gibraltar-Rif arc, with a presently active arcuate submarine accretionary wedge offshore to the west. Interpretation of present-day mantle seismic anisotropy in terms of the flow field and tomographic modelling supports these conclusions (Diaz et al., 2010).

Gutscher (2012) suggests that the segmented left-lateral fault system comprising the Alhama de Murcia fault, the Palomares fault, the Carboneras fault, the elements of the submarine trans-Alborán shear zone and the Jebha and Nekor faults form the south-eastern wall of the back-arc extended region, whilst the right lateral system represented by the Crevillente fault (LeBlanc and Olivier, 1984; Sanz de Galdeano and Buforn, 2005; Meijninger and Vissers, 2006) forms the northern wall. These two fault systems therefore act as lateral detachments or transform faults that separate the Betic wedge from different strain regimes to the north and south. Within the Betic wedge there has been NNW–SSE shortening, presumably associated with the general convergence of the African plate towards Iberia, together with the NE–SW directed extension provoked by the slab rollback. Paleomagnetic evidence supports these relative movements, showing that clockwise rotations have affected upper crustal units on the northern edge of the wedge and counter-clockwise rotations on the south side (Platt et al., 1995; Platzman, 1992; Chalouan and Michard, 2004), although Calvo et al. (1994) reported both senses of rotation in the volcanic rocks lying to the SE of the CFZ. The deformation regime implies that when the rollback started and there had been less NW–SE convergence than now, the opening angle of the wedge would have been substantially greater than we see it at present.

Gutscher (2012) estimate the late-Serravallian to early-Tortonian position of the downgoing slab to have been about 150 km NE of its present position, implying about 30–50% stretching of the Betic crust and an average rollback velocity on the order of 15–20 mm/a. This starting point is consistent with the position of the calc-alkaline volcanic arc of the Cabo de Gata and east Alborán Sea regions, the activity of which reached its peak at about that time.

SW–NE stretching of the Betic upper crust was accommodated by displacements on low-angle extensional faults affecting the basement metamorphic rocks during the middle Miocene and later via low-angle extensional faults affecting postorogenic sediments (with SW–NE displacements) often forming linked systems with nearly strike-slip transfer faults (García-Dueñas et al., 1992; Booth-Rea et al., 2004; Martínez-Martínez et al., 2006; Meijninger and Vissers, 2006; Giaconia et al., 2011). The progressive development

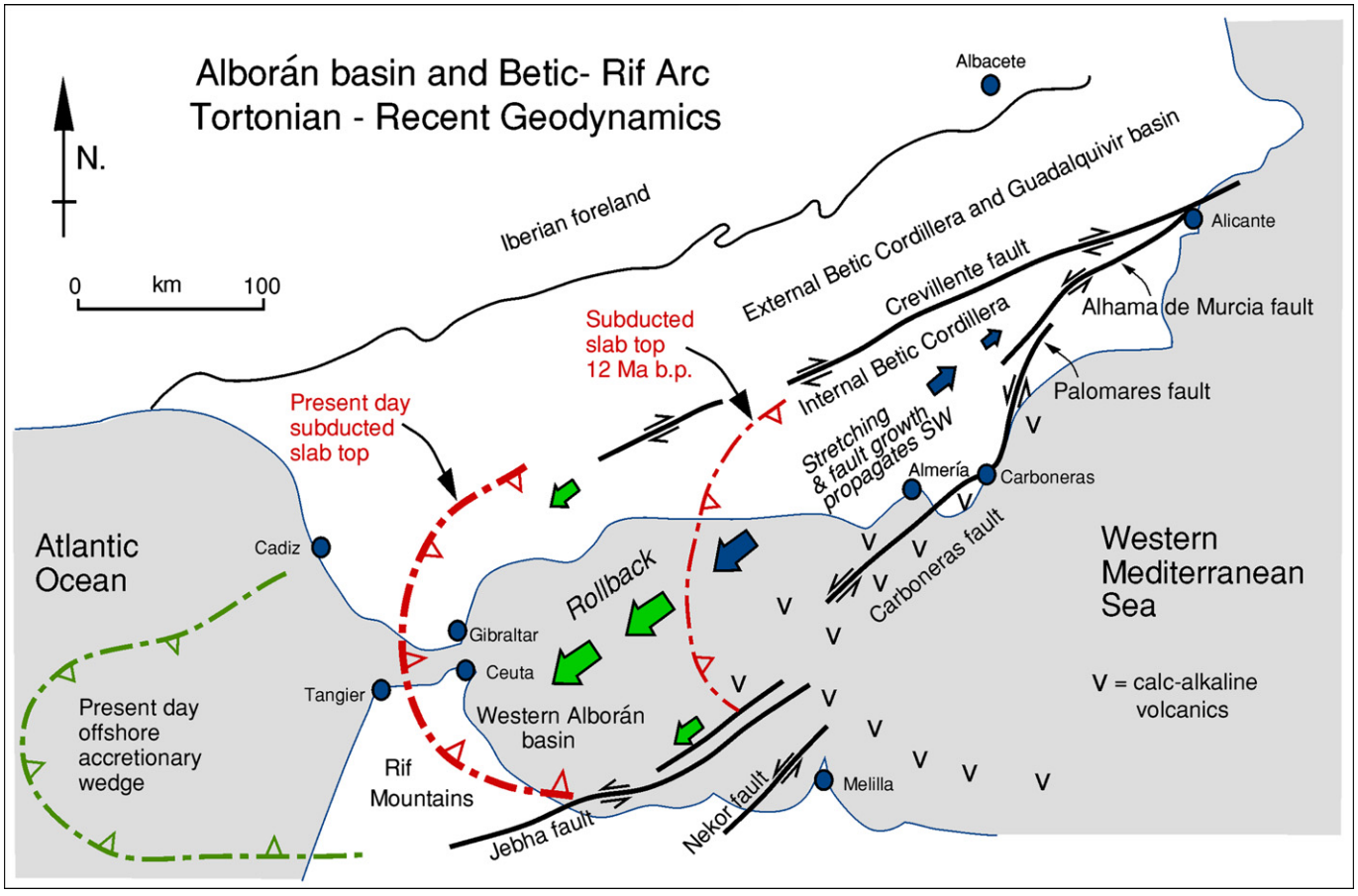

Fig. 2. Map of SE Spain and NW Africa, separated by the Alborán Sea basin, showing the geodynamic scheme (based on Lonergan and White, 1997 and Gutscher, 2012) for the Serravallian through Recent evolution. Slab rollback is accommodated by stretching within the Betic-Alborán wedge that is bounded by right-lateral and left-lateral wrench fault systems.

and evaluation of the rollback model and the role in it of the Carboneras fault system as a lateral detachment fault requires detailed information on the history and geometry of the system such as is developed in this paper.

3. The basement rocks

The structurally-lowest part of the metamorphic basement (see main map, Fig. 3) consists dominantly of upper greenschist facies graphitic mica schists and quartzites that comprise the Nevado-Filabride Complex (Kampschuur and Rondeel, 1975; Torres-Roldán, 1979; Platt and Vissers, 1989; Lonergan and Platt, 1995). These rocks display evidence of polyphase metamorphism extending to early Miocene time (Westra, 1969; Torres-Roldán, 1979; Sanz de Galdeano, 1990; Platt and Vissers, 1989; Vissers, 2012). The rocks of the Nevado-Filabride complex throughout the region are overlain tectonically by lower-grade (lower greenschist facies) phyllites with subsidiary ferruginous quartzites, in turn overlain stratigraphically by pervasively mesofractured dolomitic carbonates that are sometimes interbedded with highly tectonized gypsum (e.g. GR 593968 4099528). This association is ascribed to the Alpujárride nappe (Westra, 1969; Kampschuur and Rondeel, 1975; Torres-Roldán, 1979; Faulkner et al., 2003) and the rocks are inferred to be Triassic in age (Platt et al., 2005). This sequence is for the most part gently dipping throughout the Betic Cordilleras but is heavily dissected by erosion, such that the generally gently-dipping dolomitic unit often forms the capping on hilltops, or indeed entire upland ranges, e.g. the Sierra Cabrera (Garcia Monzón et al., 1974). Dolomites overlying non-metamorphic red sandstones and siltstones also form an additional thin tectonic slice on the southern side of the CFZ and elsewhere in the region, and have been ascribed to a highest level tectonic unit, the Maláguide unit (Lonergan, 1993). That the contact between the remains of these tectonic units outcrop at similar topographic levels to the north and south of the CFZ suggests strongly that the main movements on the CFZ are close to pure strike-slip.

The structurally highest (non-metamorphic) tectonic slice, sometimes resting directly on metamorphic basement rocks in the CFZ, contains massive carbonates and carbonate breccias bearing Cretaceous/Palaeogene fossils, and boulder beds derived from the erosion of non-metamorphic Triassic sediments. These rocks too can be ascribed to part of the Maláguide tectonic unit. These three structurally superimposed tectonic units are marked by upward stepwise decreases in metamorphic grade, which has been interpreted as evidence for superposition in an extensional tectonic regime, such that parts of the metamorphic sequence have been excised (Platt and Vissers, 1989; Lonergan and Platt, 1995).

Stratigraphic constraints require this initial stage of extensional deformation to have occurred during early Miocene times (Aquitanian and Burdigalian), and such tectonic unroofing of deeper metamorphic units helps to explain geochronological evidence for very rapid cooling and depressurization of the metamorphic pile during Burdigalian (22–18 Ma) time (Zeck, 1996, 2004; Monie et al., 1991; Platt and Vissers, 1989; Platt and Whitehouse, 1999; Vissers, 2012).

In the basement rocks near Carboneras, these generally low-angle extensional tectonic contacts (e.g. GR 596407 4098883 and

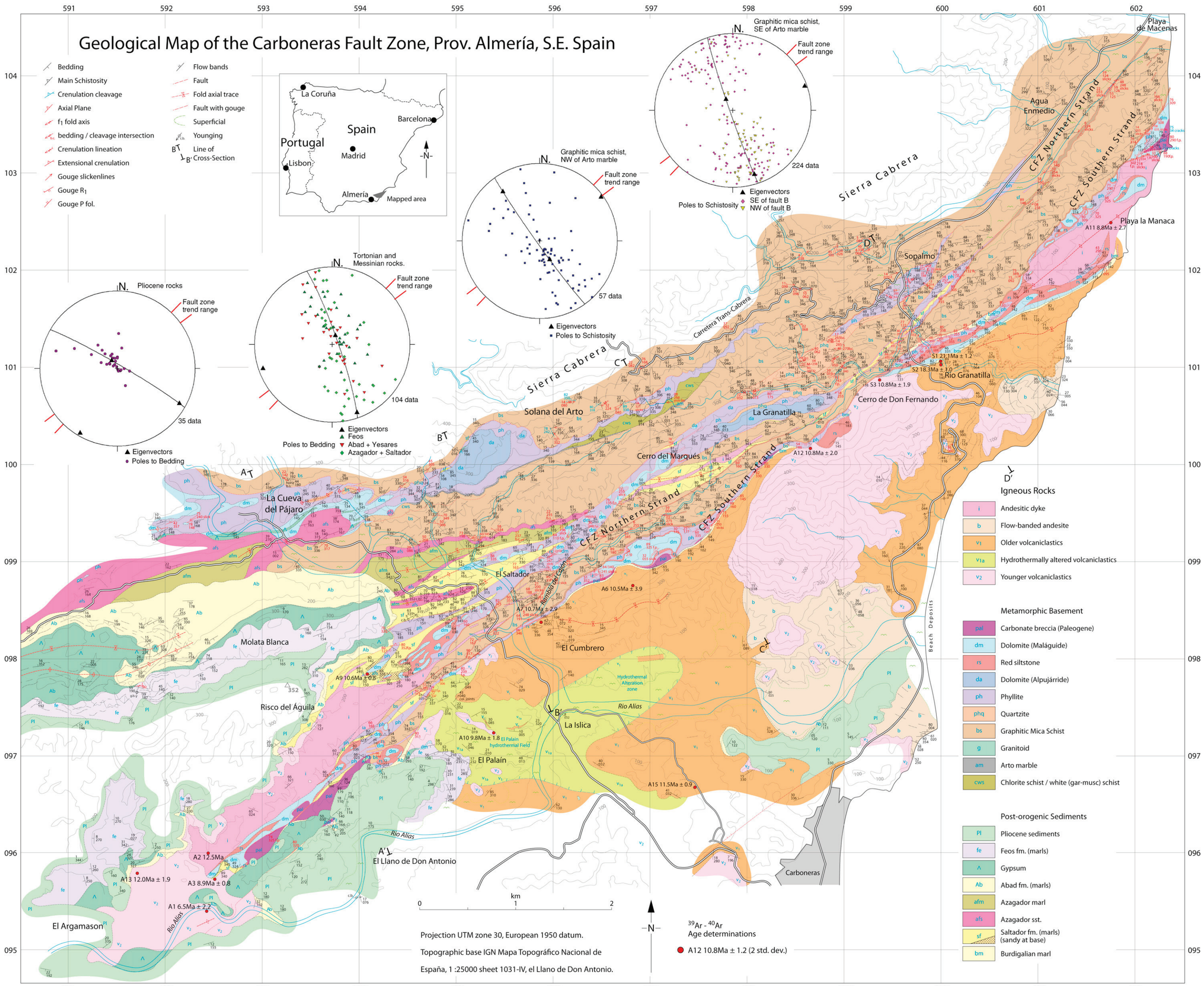

Fig. 3. Geological map of the north-eastern end of the CFZ, where fault activity affects the basement rocks. Inset lower hemisphere, equal area, lower hemisphere stereoplots show how basement schistosity and bedding in the older cover rocks are folded about axial directions that trend obliquely to the superimposed main fault trends. The same ornament is used for selenitic Messinian gypsum and the tectonized gypsum that occurs patchily with the Triassic carbonate deposits.

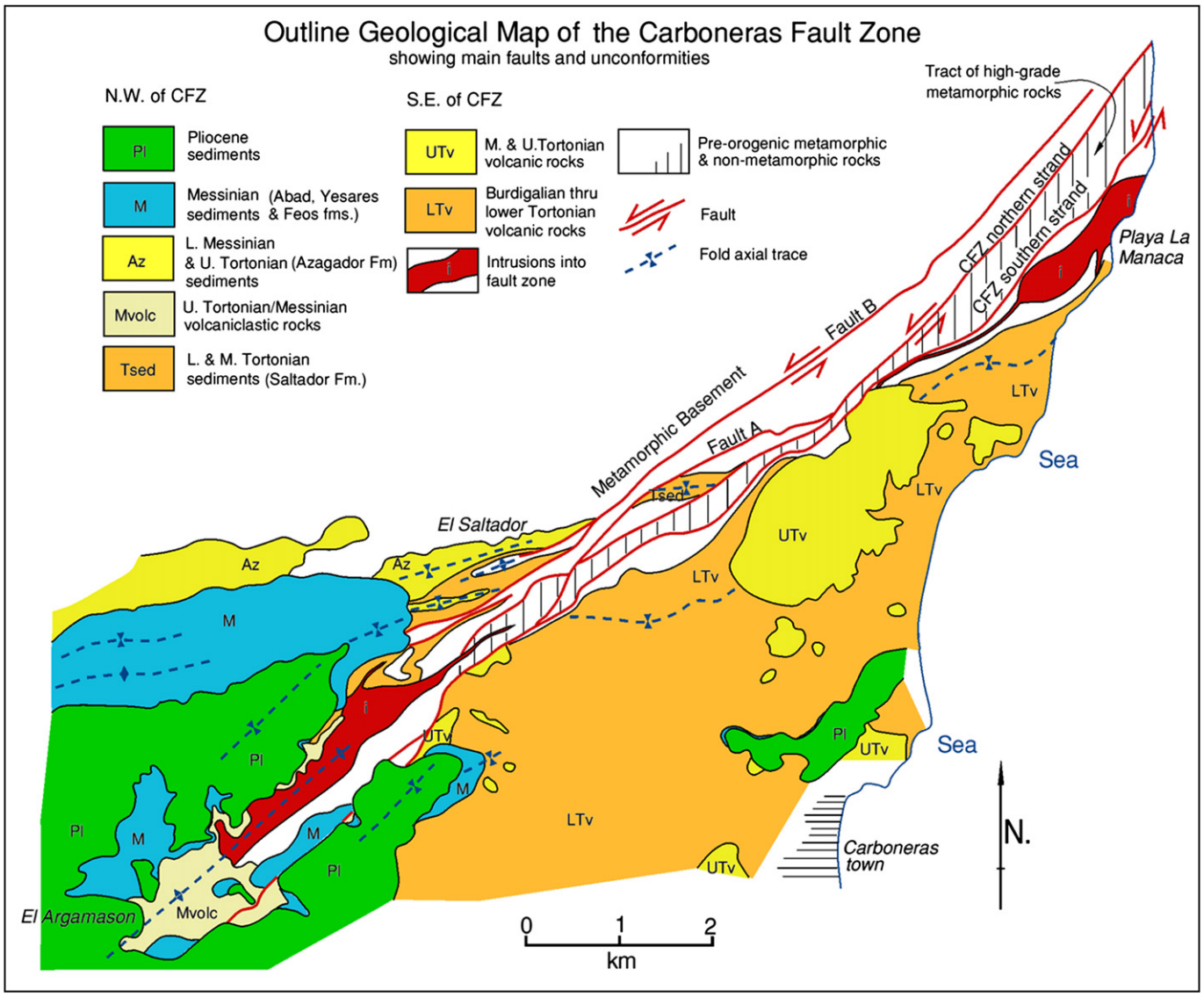

Fig. 4. Outline geological map of the CFZ, in which the area is divided into units defined by principal faults and unconformities. Messinian and Pliocene sediments are present on both sides of the CFZ. Older postorogenic rocks SE of the CFZ are represented mainly by Burdigalian through Tortonian volcanic rocks, but to the NW only by Serravallian through Tortonian marine sediments. Any previously deposited volcanic rocks to the NW of the CFZ have been removed by fault displacements and erosion. Only relatively minor strike-slip displacements have occurred since the Messinian, but the antiformal shape of the Messinian/Pliocene outcrops show that there has been transpressional uplift by about 200 m along the trace of the CFZ since early Messinian time.

594061 4097035) are often marked by low grade fault rocks, dominated by cataclastic deformation with growth of syntectonic clay minerals, indicating shearing in the uppermost few km of the crustal section. The displacements of the CFZ, on the other hand, are of younger Miocene ages than the late-orogenic extensional faulting, but texturally-similar fault rocks of the two events can sometimes be found in contact with each other, giving the impression that the CFZ rocks have a wider outcrop than is really the case (e.g. GR 597124 4099356 and 599920 4101188).

The metapelitic rocks of the basement units display a penetrative schistosity, mostly ENE trending, that is axial-planar to (rarely seen) tight to isoclinal folds of bedding in the Nevado-Filabride schists. In the phyllites and quartzites of the Alpujárride units larger-scale folds, tens to hundreds of metres in wavelength with axial-planar schistosity can be mapped (e.g. around GR 599320 4101612, on cross-section line D–D′, Fig. 7). The schistosity in both of these units was subsequently affected by the formation of an extensional crenulation cleavage mostly recording top to the north shear sense, and then folded about approximately ENE trending near-horizontal axes (Figs. 3 and 4). All of these structures are cut by NE trending faults of the CFZ, and there is no reason to believe that the formation of the folds of schistosity is directly related to the left-lateral movements on the CFZ.

4. The Carboneras fault system

The Carboneras fault system cuts all the basement rocks plus the volcanic units and almost all the components of the post-orogenic sedimentary rock sequence, although progressively younger rocks are less affected by the faulting. The CFZ in the basement rocks consists principally of two strands of fault rock (Figs. 3 and 4), respectively the northern and southern strands of the CFZ, with subsidiary fault strands between them (Fig. 3; Faulkner et al., 2003). The two bounding faults enclose a tract of

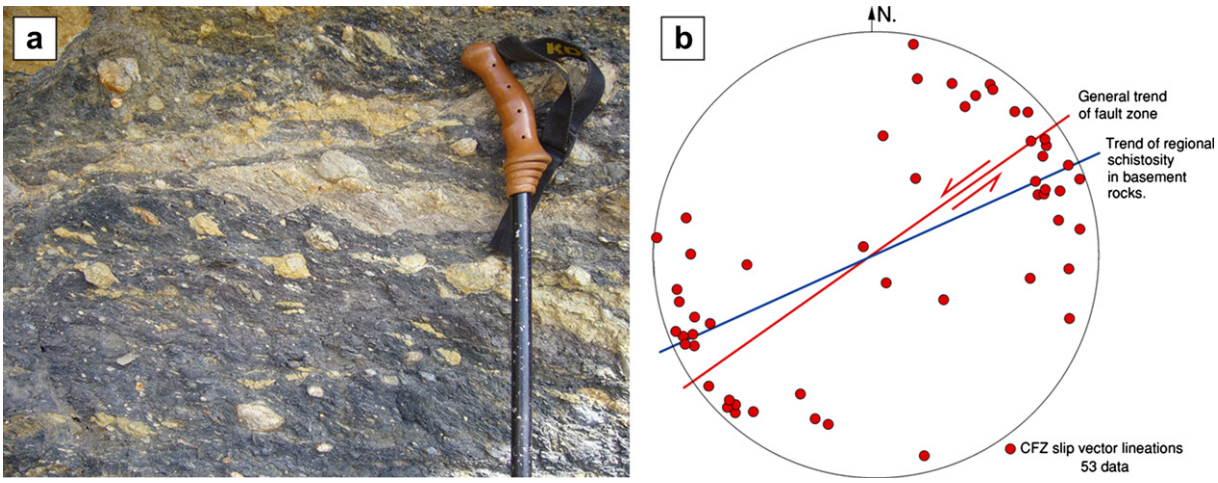

Fig. 5. (a) Internal structure of fault gouge in the Carboneras fault zone at GR 601071 4102994, looking southeastward. Primary 'P' foliation in the gouge extends top left to bottom right, with light coloured stringers and trails drawn out in the foliation. These features are cut by R_1 Riedel shears, with a left-lateral sense of displacement. (b) Slip vector determinations from throughout the CFZ, using P/R_1 orientation relationships or slickenline (mechanical wear groove) orientations. The scatter corresponds to local variations in the orientation of fault planes and foliation surfaces about the general orientation of the fault zone. Movements are all left-lateral, strike-slip.

significantly higher grade basement schists, bearing staurolite, andalusite and sillimanite, locally migmatitic with minor granitoids that yielded ~20 Ma ages (GR 597388 4099444 and 598084 4099960) (Platt and Whitehouse, 1999). Incorporation by strike-slip movements of these distinctive basement rocks between the two main faults of the CFZ over a distance of more than 10 km suggests that these fault strands have accommodated the largest displacements within the CFZ. To the north of these principal strands are two further long faults (here called fault A and fault B on Fig. 4 – to avoid any confusion with names used in earlier literature) that cut the older part of the postorogenic sedimentary sequence. They appear to have smaller displacements than the two main Carboneras faults (totalling ~2 km on faults A and B, from displacement of the synclinal fold structure affecting Tortonian marls from the vicinity of El Saltador village (GR 595824 4099228) to the south flank of Cerro del Marques (GR 597188 4099904)). These latter faults may be slightly younger than the two main strands of the CFZ, because they are straighter, but the northern strand of the CFZ also cuts the U. Serravallian/L. Tortonian marls of the Saltador Formation.

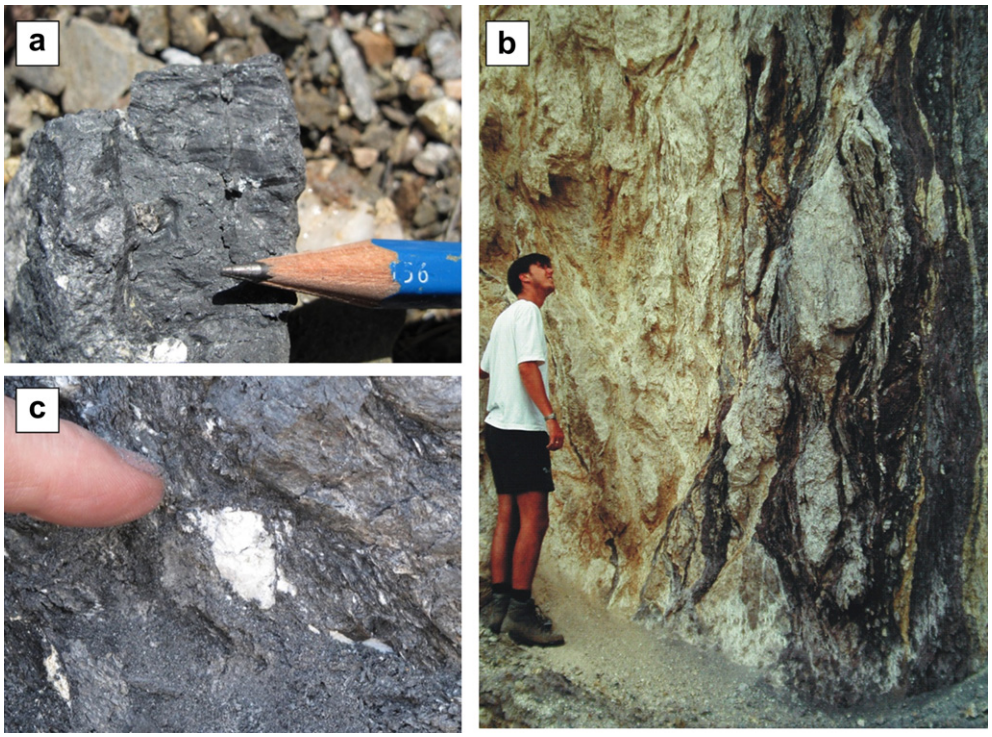

Fig. 6. Features of fault gouge. (a) Mechanical wear grooves (parallel to pencil point) on 'P' foliation surface of graphitic mica schist-derived fault gouge at GR 601071 4102994. (b) Example of a pulverized clast of white vein quartz in clay-bearing gouge derived from graphitic mica schist at GR 594264 4099110. The pulverized clast falls to a fine powder if disturbed, yet the near-equant overall shape suggests little finite strain has been accumulated. (c) Internal structure of fault rocks within the northern strand of the CFZ at GR 599569 4101238, looking NE. To the right phyllite-derived gouge (dark) displays a vertical foliation and included slabs of pulverized quartzite. To the left is cataclasite derived from the extreme fragmentation of sandstone.

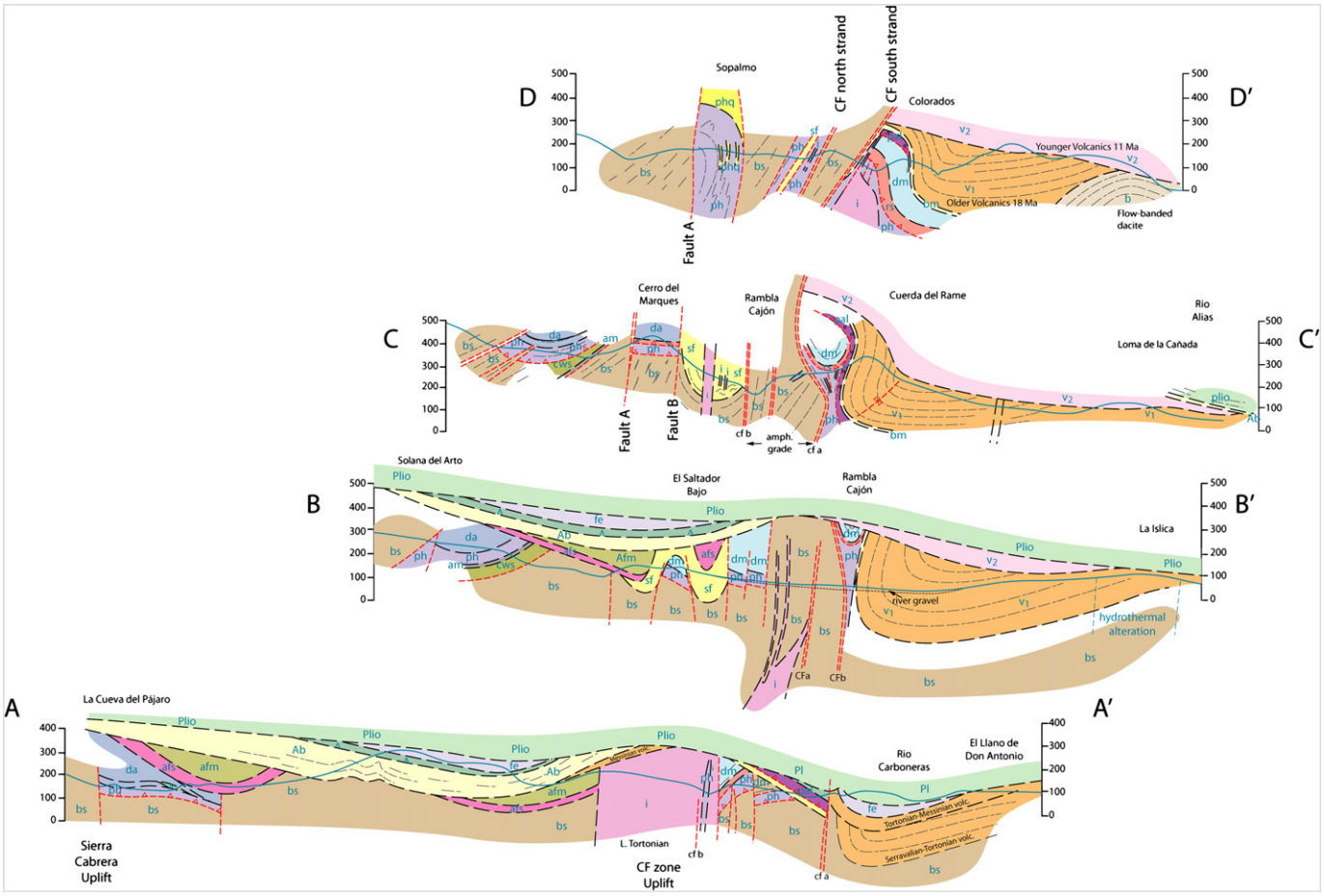

Fig. 7. Cross sections (vertical and horizontal scales equal) each looking NW along the lines indicated on Fig. 3. Alphameric key to formations corresponds to that used in Figs. 3 and 9. Messinian through Pliocene formations are uptilted along the flank of the Sierra Cabrera to the north, and are also arched over the CFZ, indicating that the strike-slip movements also involve transpression.

The main displacements of the northern and southern strands of the CFZ are accommodated in fault gouge zones a few metres wide, principally derived from graphitic mica schist. These display spectacular internal structuring showing P/R_1 foliation (Rutter et al., 1986) relations that unequivocally indicate left-lateral strike-slip displacement sense (Fig. 4). Within the fault gouge, at the grain-scale feldspars and mechanically degraded micas are transformed to variably oriented clay minerals (Rutter and White, 1979; Rutter et al., 1986; Solum and van der Pluijm, 2009). The fault rock often displays fine-scale frictional wear slickenlines on the gouge foliation surfaces (Fig. 5) and evidence of solution and redeposition (pressure solution) of embedded quartz clasts in the clay + mica matrix (Rutter and White, 1979; Rutter, 1983). These syntectonic mineral growth features in the fault gouge indicate that the microstructure was produced mainly by slow creep processes, which will also tend to obliterate any sharp, seismogenic slip surfaces that might have developed. The fault gouge mineralogy and frictional/brittle deformation features indicate that all fault activity occurred entirely in the uppermost 5 km or so of the crust.

Bearing in mind that there was insertion of a slab of high-grade metamorphic rocks between the two main (northern and southern, Figs. 3 and 4) CFZ fault strands, it is striking that there is no evidence of preservation of deeper-level mylonitic fault rocks that would explain the mechanics of incorporation of the high grade schists into their present level during early Miocene time. The present CFZ must have cut through and displaced basement rocks that had already been moved into a shallow crustal level.

X-ray diffraction (XRD) analysis of clay-bearing fault gouges shows the Nevado-Filabride schist-derived gouges to be dominated by chlorite, muscovite and quartz, with traces of dolomite, kaolinite, illite and feldspar. Fault gouge derived from Alpujárride phyllite is dominated by chlorite, illite and muscovite, with hematite and traces of dolomite, calcite, feldspar and quartz.

4.1. Other fault systems

Stapel et al. (1996) and Booth-Rea et al. (2003) show a Gafarillos fault outcropping 6 km WNW from La Cueva del Pájaro, with a WNW–ESE trend and forming the southern margin of the Sorbas basin but with a right-lateral sense of movement, and regarded it as a conjugate fault to the CFZ. Other authors have suggested this has a prolongation eastwards that forms part of the CFZ and lies to the NW of our Fault B (Keller et al., 1995; Huibregtse et al., 1998). Fortuin and Krijgsman (2003) and Van der Poel (1992) show a lateral extension of the faulting that passes through Polopos (10 km to the west of Fig. 4) passing through basement schists substantially to the north of the area on Fig. 4. Faulting that cuts the basement NW from the CFZ is likely to form part of the network that accommodates NE-SW extension within the Betic-Alborán belt.

Our map (Fig. 3) shows that in the vicinity of Cueva del Pájaro a slab of generally south-dipping phyllites and dolomites of the Alpujárride tectonic unit lie upon graphitic mica schists (although the contact is locally overturned) of the Nevado-Filabride unit with

low-grade fault gouge developed at the contact. Against the southern edge of the Alpujárride rocks, as a unit within the Nevado-Filabride complex lies a tract of white garnet-muscovite schist, chloritic shists and a banded calcite marble that together comprise the Arto complex of Westra (1969). This tract of fault-bounded blocks and unusual basement rock types is unconformably overlain by the U. Tortonian/L. Messinian Azagador sandstone unit, therefore we infer that these fault contacts were developed as part of the early Miocene extensional faulting activity, rather than forming part of the U. Miocene CFZ. However, along the northern edge of the outcrop of Alpujárride rocks lie slivers of marls of the Tortonian Saltador Fm. (e.g. GR 594896 4099936), implying that some minor fault movements, perhaps reactivating pre-existing faults, occurred in this zone and was coeval with the main CFZ activity.

Giaconia et al. (2011) demonstrated the existence of NE–SW directed, low-angle, synsedimentary extensional faulting active during Tortonian time in the nearby Sorbas basin to the NW. Individual extensional faults are hard-linked to each other via NE-SW trending strike-slip faults that are therefore of similar orientation and character to the CFZ. The CFZ, however, is a much longer system that, as amplified below, also features important magmatic activity of subcrustal origin, and should be regarded as a separate tectonic feature in its own right.

4.2. Pulverized clasts

In many places in the graphitic mica schist-derived fault gouges, fragments up to 5 cm diameter of white vein quartz, derived from the protolith, are found embedded in the black, clay-bearing fault gouge. These display varying degrees of pulverization such that in the most extreme state they are intensely fractured, falling to a powder of submillimetric particles if agitated (Fig. 6b). There is no obvious preferred orientation of the fractures in the clasts. Despite the highly fractured state, the vein quartz clast shape is usually near equidimensional, suggesting that little finite strain has been involved in the fragmentation process. This feature has been observed in other fault zones, prompting the suggestion that the damage arises from seismogenic stress waves passing through the rocks (e.g. Ben Zion and Shi, 2005; Billi and Di Toro, 2008; Mitchell et al., 2011), and hence that these features could be regarded as paleoseismic indicators. In contrast, the microstructural features indicative of gouge flow, accompanied by low-grade metamorphic reactions that result in growth of clay minerals, pressure solution, and an apparent tendency for gouge zones to widen rather than becoming more and more localized into a narrow zone, suggest that the aseismic creep is the dominant mode of displacement accumulation, perhaps punctuated by periodic seismogenic events on the faults locally developed in the more competent units such as the dolomites (Faulkner et al., 2003).

4.3. Effects of the faulting activity on the basement rocks

Apart from shear displacements across the faults of the CFZ, cutting across the schistosity and folded schistosity, there are often wide zones of cataclastic damage extending into the basement rocks for tens of metres on either side of the fault strand cores. Damage occurs on a wide range of scales of crack length, the longest of which disrupt the rock mass into blocks of metric dimensions that are displaced slightly against each other. In some cases the regional schistosity is deflected noticeably towards the main fault planes, e.g. in the sliver of country rock between the northern and southern strands of the CFZ near the coast.

5. The volcanic rocks

The (mainly) amphibole- and feldspar-phyric andesitic-dacitic volcanic rocks of the Cabo de Gata series include extrusive lavas and a wide range of volcaniclastic rocks. The CFZ itself (Fig. 4) also hosts two substantial elongate intrusive bodies (on either side of the CFZ southern strand, centred on GR 593460 4097048 and GR 601572 4102220). These are several km long and up to 500 m wide. In addition, there are many vertical, thin (up to 5 m wide), NE–SW trending andesitic dykes that intrude the CFZ, which has acted as a conduit bringing intrusive rocks up to the surface. The Serrata ridge, lying some 10 km to the SW of the area mapped (Fig. 1) is a prominent uplift of intrusive and volcaniclastic rocks in the CFZ that is 7 km in outcrop length. At its north-eastern extremity basement phyllites and dolomites are lifted and arched over the top of an intrusive body, forming its roof. This is geometrically similar to the antiformal arching of basement and sedimentary cover rocks over the massive intrusive body that outcrops on the coast, at the north-eastern extremity of the CFZ (Figs. 3 and 4). We infer that eruptive centres developed along the trace of the CFZ, but any surface edifices have since been removed by erosion. Thus the rocks of the Cabo de Gata volcanic series play an important role in the evolution of the CFZ, and they are not to be regarded simply as older rocks cut by the faults of the CFZ.

5.1. Dating of the volcanic rocks

During this study we have obtained 11 new ^{40}Ar–^{39}Ar radiometric dates from amphibole crysts in the volcanic series (summarized in Table 1 together with our previously reported dates in Scotney et al., 2000, and shown in map view on Fig. 3). These dates help to constrain movement periods on the CFZ.

Amphibole separates were prepared by lightly crushing bulk rocks, followed by hand-picking grains under a binocular microscope. Samples were washed in deionized water and acetone and dried under an infra-red heating lamp. Between 0.009 and 0.0012 g of samples were weighed, wrapped in aluminium foil and sealed in quartz ampoules together with the flux monitor Hb3gr ($t = 1073.6 \pm 5.3$ Ma, Jourdan et al., 2007). Nuclear irradiation was carried-out in position B2W of the SAFARI-1 reactor at Pelindaba, South Africa with a fast fluence of $\sim 2 \times 10^{18}$ n cm^{-2}. Argon was extracted from the samples using a Ta resistance furnace over the temperature interval 400–1600 °C using 30 min heating steps. The Argon was purified using a SEAES NP10 getter at 250 °C and transferred to the MS1 mass spectrometer for isotopic analysis. Blank levels were determined at three temperatures during the course of the experiments, in units of 10^{-15} mol ^{40}Ar, these were: 22 ± 4 (600 °C); 40 ± 9 (1000 °C) and 97 ± 20 (1400 °C). Blank corrections were typically ~10% of most argon release steps. Raw data were corrected for blanks, mass discrimination (calibrated using atmospheric argon), radioactive decay and neutron interference. The latter were determined from pure CaF_2 and K_2SO_4 salts included in the ampoule with the following values: $(^{40}Ar/^{39}Ar)_K = 0.026 \pm 0.023$; $(^{38}Ar/^{39}Ar)_K = 0.01243 \pm 0.00002$; $(^{39}Ar/^{37}Ar)_{Ca} = 0.000666 \pm 0.000003$; and $(^{36}Ar/^{37}Ar)_{Ca} = 0.000267 \pm 0.000007$. ^{40}Ar–^{39}Ar stepped heating data and age spectrum diagrams are given in the Supplementary Data Table 1 and Supplementary Data Figure 1. All ages are reported at the 2σ level of uncertainty. Age spectrum and isotope correlation diagrams were produced using the Isoplot/Ex3.23 program (Ludwig, 2003).

Age determinations coupled with stratigraphic relations show that the volcanic rocks can be divided into two groups: an older group formed between 18 and 13 Ma (Burdigalian–Serravallian)

Table 1
$^{40}Ar-^{39}Ar$ radiometric ages on amphiboles from igneous rocks of the Cabo de Gata volcanic series. Uncertainty estimates are given as ±2 standard deviations.

Spec. Nr.	Location (GR) easting/northing	Age BP (Ma)	Rock	Comment
A1	592488 4095381	6.5 ± 2.2	Volcaniclastic 500 m E of El Argamasón.	
A2	592463 4095938	12.5 ± 1.9	Centre of thick andesite dyke.	
A3	592502 4095718	8.9 ± 0.8	Volcaniclastic S of CFZ near el Argamasón.	
A6	596850 4098730	10.5 ± 3.9	Volcanic breccia.	
A7	595860 4098350	10.7 ± 2.9	Volcanic breccia.	
A9	594090 4097840	10.6 ± 0.8	Andesite dyke cutting basal Saltador Fm.	
A10	595390 4097240	9.8 ± 1.8	Outlier of red (younger) volcs. near Minas El Palaín.	
A11	601800 4102550	8.8 ± 2.7	Massive intrusive andesite near La Manaca beach.	
A12	598600 4100150	10.8 ± 1.6	Andesitic breccia near CFZ southern strand.	
A13	591640 4095820	12.0 ± 1.9	Andesitic breccia beneath gypsum, El Argamasón.	
A15	597420 4096650	11.5 ± 0.9	Cañada de Don Rodrigo, near Carboneras.	
SP1	599950 4101040	21.1 ± 1.2	Amphibole crystals in tuff, R. Granatilla.	
SP2	600010 4100997	18.3 ± 1.0	Volcaniclastic breccia, R. Granatilla.	
SP3	599350 4100870	10.8 ± 1.9	Volcaniclastic breccia, Younger volcanics on Cerro de Don Fernando.	

and which were deposited before the CFZ was active, and a younger, unconformable group formed between 13 and 6 Ma (Serravallian–Messinian), during the main stage of activity of the CFZ.

5.2. Stratigraphy of the volcanic rocks: the older group

The oldest in-situ volcaniclastic rocks (18 Ma, GR 599998 4100992) lie to the SE of the CFZ and are tilted to the vertical against its southern strand. They are roughly coeval with the metamorphic peak in sillimanite grade basement rocks against which they are now juxtaposed by fault movements (GR 598076 4099956). These volcaniclastic rocks represent the oldest eruptive rocks of the region surviving *in-situ* and are immediately underlain by thin bands of calcareous rock bearing volcanogenic clasts interlayered with marine marls that were dated using microfossils by Serrano (1990b) at about 16.5 Ma. The reason for the 1.5 Ma discrepancy with the microfossil age is unclear, but the tectonized state of the marl would make it difficult to recover a good-quality fauna. The water-lain tuffaceous bands (GR 599998 4100992) also contain fragments of dolomite and red siltstone of the Maláguide basement rocks, and redeposited amphiboles that yield an age of 20 Ma (Burdigalian, Scotney et al., 2000). Thus there is evidence of some surficial volcanic activity at the same time that the basement complexes were undergoing active extensional tectonics. The base of the thin (20 m) band of Burdigalian marls makes an unconformable contact to the NW with Maláguide basement rocks and can be traced from the coast at GR 601540 4101880, some 7 km southwestwards to GR 596484 4098940, where it is overstepped by stratigraphically overlying volcaniclastic rocks. At various points along the outcrop of the stratigraphic top of the Burdigalian marl, small clasts of pyroxenite and cumulate gabbro were found (e.g. GR 598184 4099988), which may have a lower-crustal origin. These are inferred to have been ripped from the walls of the igneous conduits at an early stage in the evolution of the volcanic complex.

The volcanic rocks adjacent to the coastline consist of thick (up to 50 m), often irregularly shaped volcaniclastic units (lahars, agglomerates, extrusive lavas and minor intrusives), but it is clear that they are sharply tilted to the vertical (and locally overturned) against the SE side of the CFZ, suggesting that the CFZ has a transpressive character (Fig. 7). Serrano (1990a,b) reported a microfossil age of U. Langhian/Serravallian (13.5 Ma) from vertically-tilted marls interlayered with volcaniclastic rocks at GR 595476 4098188, which is consistent with the inferred structure of the volcaniclastic series to the south of the CFZ, and implies that the first movements on the CFZ did not start prior to the mid-Serravallian stage.

5.3. Stratigraphy of the volcanic rocks: the younger group

Within the volcanic sequence is a substantial angular unconformity that is well displayed on the beach at La Galera (GR 599668 4096968), at GR599632 4098480 and GR 594852 4097380 (Figs. 8 and 9). The volcanic rocks above the unconformity are usually more strongly red-weathering than those beneath, which are often grey-green weathering with a stronger tendency to hydrothermal alteration. The red volcaniclastic rocks are less severely tilted against the southern edge of the CFZ.

The younger volcanic series includes the Brèche Rouge (Serrano and Gonzáles Donoso, 1989; Uwe et al., 2003), characterized by volcaniclastic breccias with the inter-clast volumes infilled with a pink, muddy carbonate matrix rich in micro- and macrofossils that yield mid-Tortonian ages (8–9 Ma). These breccias are well-displayed at GR 594824 4097400 and 598228 4095592. However, $^{40}Ar-^{39}Ar$ ages on amphiboles suggest a substantial part of the volcanic rocks of the Carboneras area accumulated between 13 and 10 Ma (Fig. 3), that is mid-Serravallian through mid-Tortonian time. The earliest younger (red) volcanic rocks are tentatively ascribed to ages 11 or 12 Ma (mid-Serravallian) and younger, and this unconformity is inferred to date the start of the main movements on the CFZ, because all older volcanic rocks are tilted to the vertical against

Fig. 8. The Tortonian angular unconformity in the volcanic rocks SE of the CFZ at GR 599642 4098487 (mouth of the Rio Alías, looking north), placing red-weathering agglomerates above grey/yellow weathering agglomerates and banded tuffs. (For interpretation of the references to colour in this figure legend, the reader is referred to the web version of this article.)

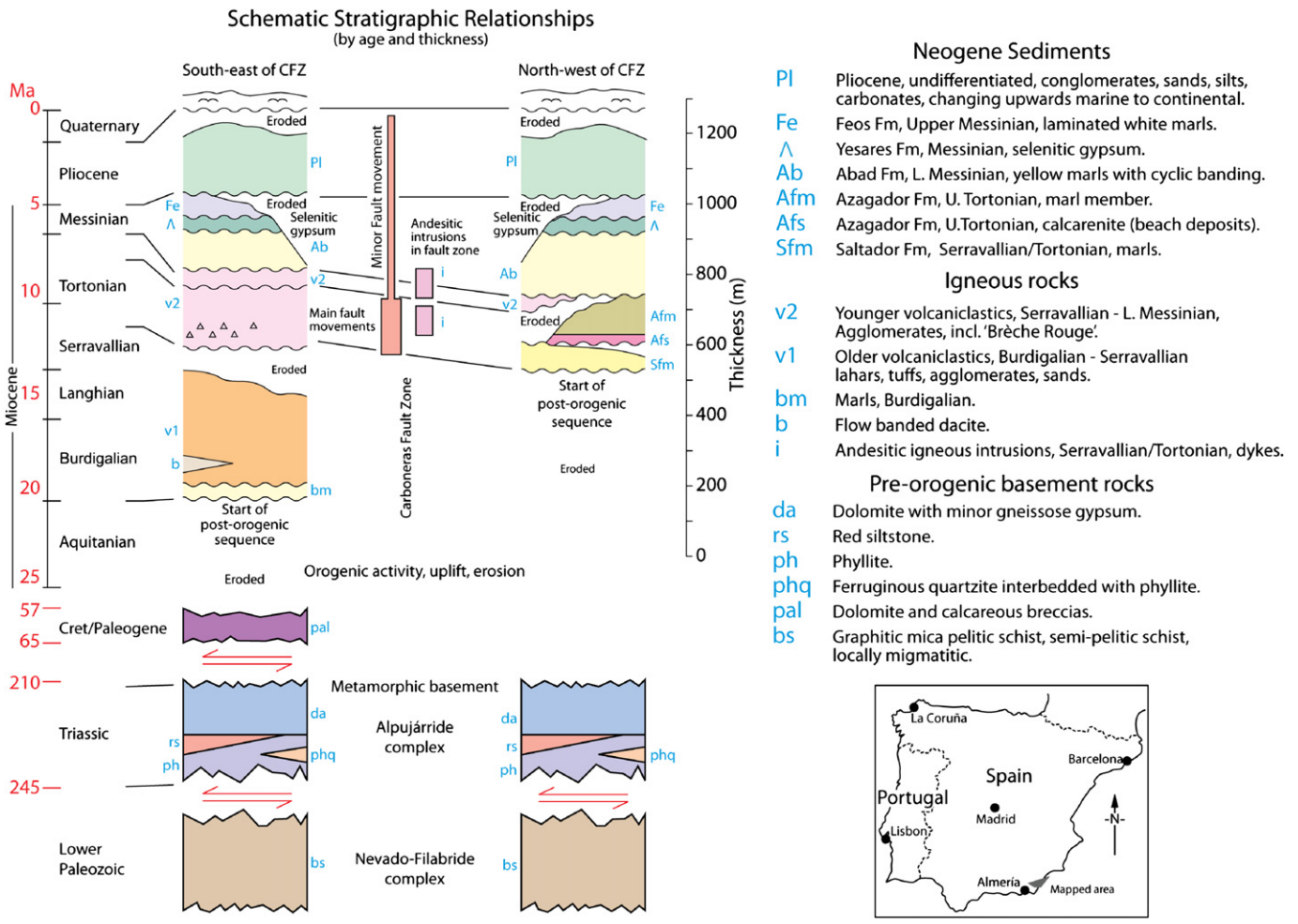

Fig. 9. Stratigraphic relationships in the Carboneras Fault Zone, showing the different post-orogenic stratigraphic sequences developed on either side of the fault zone. The different components of the basement rocks are separated by low-angle extensional faults, active mainly during Aquitanian and lower Burdigalian time.

the fault zone or are cut by it. The younger volcanic rocks overstep the base of the older volcanic rocks, onto the underlying, up-tilted Maláguide basement rocks, only to be truncated by the fault rocks of the southern strand of the CFZ (at Cerro de Don Fernando, GR 599320 4100828). Fault movements therefore continued after 10 Ma.

It seems likely that that the base of the red group is not everywhere of the same age in the region. This is illustrated by the tract of country between GR 594836 4097612 and 597152 4097824 that lies in the outcrop of the older volcanic rocks and is very strongly hydrothermally altered. It hosts the gold mineralization of El Palaín and La Islica (GR 595452 4097160 and 596368 4097304) (Morales Ruano et al., 2000; Carrillo Rosúa et al., 2002). A few 100 m west of El Palaín mine, prominent red outliers of the younger (Brèche Rouge lithotype, 9 Ma), unaltered volcanic rocks outcrop on top of the hydrothermally altered rocks.

Measured ages from the igneous intrusions into the fault zone range from 12.5 to 8.8 Ma and seem to be broadly coeval with the main period of movement of the CFZ. Waning volcanic activity continued until 6.5 Ma (L. Messinian), when 1 km east of El Argamasón there was an overstep by a thin (50 m) layer of volcaniclastic rocks right across the CFZ and towards the north-west, where they are buried beneath younger Messinian and Pliocene deposits. Otherwise, the volcanic rocks are now entirely confined to the southeast of the CFZ.

6. The post-orogenic sediments

We base our description of the stratigraphy upon formation names used by Fortuin and Krijgsman (2003) and Van der Poel (1992) for this area, but with some modification. The stratigraphic scheme for the area, emphasizing the differences in sequence to the north and south of the CFZ is shown in Fig. 9.

Whereas to the south-east of the CFZ post-orogenic sedimentation began at 18 Ma (Burdigalian), to the north of the northern strand of the CFZ the oldest sediments are U. Serravallian/L. Tortonian marls (Saltador Fm., 11 Ma and younger, based on microfossil evidence, Van der Poel (1992), Huibregtse et al. (1998), Fortuin and Krijgsman (2003)). They outcrop around the village of El Saltador (GR 595232 4098872) and sit with unconformity on basement schists and dolomites that were previously affected by some fault activity (Fig. 7). They are broadly equivalent to the Chozas Fm of the Sorbas basin (Mather et al., 2001). Thin turbiditic sands occur in the upper part of the Saltador Fm (GR 594644 4098688), and the basal part is locally sandy (GR 594072 4097840). At the latter locality these rocks are cut by an andesitic dyke that gives a $^{40}Ar-^{39}Ar$ age of 10.5 Ma (Fig. 3). 20 km further west towards the town of Nijar, but still north of the CFZ, the oldest post-orogenic rocks lying unconformably upon the basement units appear to be slightly older (Serravallian, Serrano, 1990a,b).

Rocks of the Saltador Fm. are strongly deformed into upright isoclinal folds on the order of 200 m wavelength, trending about 10° closer to east-west than the faults of the CFZ (Fig. 3), and plunge gently to the west-south-west. The faults of the CFZ cut the folds, for example the synformal inlier of rocks of the Saltador Fm lying immediately to the south of Cerro del Marqués (GR 596942 4099982) that is cut by Fault A to the NW and the CFZ northern strand to the SE. This synform is also cut by several andesitic dykes. Slivers of the Saltador Fm marls and sandstones are strung out along the northern strand of the CFZ from this synform for a distance of 5 km to the NE (Fig. 4).

The Saltador Fm is overlain unconformably by high energy, fossiliferous beach sands (Azagador sandstone of the Turre Fm of Völk and Rondeel, 1964) that overstep the Saltador Fm to the north to rest directly on basement metamorphic rocks. This is a regionally important unconformity, that can be traced west and north over the antiformal arch of the Sierra Cabrera to south side of the Vera basin (Booth-Rea et al., 2004). The Azagador sandstone passes upwards into a marly member, and they (U. Tortonian/L. Messinian) are locally unconformably overlain by the Abad marl (L. Messinian), which is rich in marine microfossils. At the western end of the area mapped, where the Abad marl oversteps directly onto the Azagador sandstone, the most detailed stratigraphic studies of the Abad marl have been reported (Sierro et al., 2001), and perhaps for this reason the Azagador sandstone and the Abad marl have previously been grouped together as members within the Turre Fm. However, the unconformity at the base of the Abad marl (7.2 Ma, Krijgsman et al., 2001; Sierro et al., 2001) means that it cannot be grouped with the Azagador sandstone therefore we will regard it as a separate formation. The Abad marls have received a great deal of attention because everywhere they show a characteristic cyclicity, with 55 alternating hard and soft bands that are attributed to astronomically controlled variations in regional climate (Sierro et al., 2001).

The Abad marls pass upwards (6.0 Ma, Krijgsman et al., 2001) into the middle-Messinian Yesares Formation, which is dominated by massive selenitic gypsum, produced by evaporation during the Messinian desiccation of the Mediterranean basin (Van der Poel, 1992; Martín et al., 1999; Krijgsman et al., 2001; Fortuin and Krijgsman, 2003; Braga et al., 2006). The evaporites are of laterally variable thickness, and are sometimes replaced by collapse breccias (e.g. GR 593584 4097868 and 592243 4097999). On the south-eastern side of the CFZ near El Argamasón (GR 591756 4095020) the Yesares Fm dips towards the south-east, and rests directly on L. Messinian volcaniclastic rocks instead of on Abad Marl. Some 2 km further north, the Messinian volcanclastic rocks are missing, and the Yesares Fm rests directly upon Abad marl.

The Messinian gypsum deposits have never been buried sufficiently (about 1 km) to cause dehydration, as evidenced by the preservation of the primary evaporitic textures. In contrast, the gypsum patchily found interbedded with Triassic dolomites and siltstones has been through burial, dehydration and the Alpine orogenic cycle, resulting in strongly deformed gneissose fabrics being produced.

The gypsum deposits of the Yesares Fm. are overlain by the Feos Fm (U. Messinian, 5.67 Ma, Krijgsman et al., 2001), dominated by white, well-bedded marls with a distinctive black, Mn-oxide rich horizon at the base. These have a much more restricted fauna, and have been interpreted as representing emergence and the transition to continental conditions, as implied by the name 'Lago-Mare facies' (Fortuin and Krijgsman, 2003). Whilst there is great variation in facies and depositional conditions represented by the sequence of Messinian formations – Abad, Yesares and Feos, from the point of view of the influence of the package on structural geometry they are almost conformable to each other (Fig. 9).

Whilst the Tortonian rocks of the Saltador Fm show the effects of tight to isoclinal folding almost everywhere, the younger sedimentary units are also affected by significant folding. At GR 594276 4099102, between the villages of El Saltador and Cueva del Pájaro, post-orogenic sediments of the overlying Azagador Fm that are affected by folding can be seen resting unconformably upon basement schists bearing pre-existing fault gouge zones. To a large extent, the folding in the cover rocks is thought to be accommodated by movements along small fault slivers in the basement rocks, producing bend folding. However, there is also evidence of NW-SE directed shortening in the cover rocks because within the Azagador Formation (e.g. at GR 594590 4099098 and 594546 4098714) a weak tectonic cleavage, axial planar to the host fold, has formed by mechanical rotation of lithic fragments of schist within the mechanically weak and porous sandstone.

The Messinian units are also locally affected by significant folding (Fig. 3) in addition to being arched over the trace of the CFZ. In the west-central part of Fig. 3 the Abad marls and the Yesares gypsum are folded into an east-west trending synform-antiform pair (centred on GR 591856 4098088) with vertical axial surfaces and half-wavelengths of around 200 m. At this locality the antiform is almost isoclinal in the Abad marl, with many metre-scale minor folds, but becomes less tight further west and east. It is not clear what has caused these folds to develop, for this area is 2 km away from the immediate influence of the CFZ. Their development may be influenced by displacements on other, then-active faults in the basement that are not directly seen, but they testify to continuing NNW-SSE shortening through the Messinian.

A marked angular unconformity separates the Messinian formations from the overlying Pliocene rocks, that represent a marine incursion at the base (4.8 Ma), followed by several hundreds of metres of fan-delta sediments that record emergence and uplift.

To summarize the history of the post-orogenic sediments north and west of the CFZ (Figs. 4 and 9): there are 4 major unconformities :

(a) At the base of the L. Tortonian Saltador marl formation. These are the first post-orogenic sediments to the NW of the CFZ.
(b) At the base of the Azagador sandstone, which oversteps northwest onto the basement rocks.
(c) At the base of the Abad marl, which oversteps northward onto the Azagador sandstone.
(d) At the base of the Pliocene formations.

On Fig. 4 these unconformities and the main strands of the CFZ are highlighted.

Towards the northwest, these unconformities are clearly a consequence of the episodic uplift of the Sierra Cabrera lying to the north as an antiform from latest-Tortonian time onwards, but along the trace of the CFZ these unconformities are due to coeval episodes of uplift of the basement rocks of the fault zone (see map (Fig. 4), cross sections (Fig. 7) and the stratigraphic scheme (Fig. 9)). Each of the main units bounded by unconformities at the base is progressively less severely arched over the CFZ. Thus the overall shape of the outcrop pattern of the post-orogenic sediments from the CFZ north-westwards is dominated by the SW plunging antiformal arch over the CFZ, and the SW plunging synformal zone in the sedimentary cover, extending south-westwards from El Saltador.

The uplift of the CFZ that is recorded by the unconformities in the post-orogenic sediments in the study area is also recorded in the decreasing impact of strike-slip fault displacements in the same rocks. The only effects of discrete fault displacements on Pliocene rocks are at GR 592912 4095636 (2 km east from El Argamasón, GR

591104 4095384), where Pliocene sediments are displaced against Messinian gypsum. Although the amount of offset is unclear, it cannot be more than tens of metres horizontally and vertically. There is some indication that locally the younger Pliocene rocks overstep the fault contact. However there is an important general uplift and emergence during Plio-Quaternary time recorded by the distribution of topographic height of these systems and river terracing (Martin et al., 2003; Maher and Harvey, 2008), and this is modulated by the localized arching of Pliocene rocks over the CFZ, which must be related to movements on the CFZ.

From the Serrata ridge and further SW along the CFZ outcrop a number of studies have drawn attention to apparent left-lateral stream offsets (Boorsma, 1992; Bell et al., 1997; Reicherter and Reiss, 2001), submarine offset features (Grácia et al., 2006), and displacements of beach deposits (Bell et al., 1997) and these have been interpreted in terms of relatively recent activity of the faults of the CFZ and the trans-Alborán shear zone. They may point to a migration of activity towards the SW with time.

7. Geological structure and history of the basement rocks south of the CFZ

The pre-CFZ history of the basement rocks south of the southern strand of the CFZ developed in a region relatively further south-west, laterally separated from rocks north of the fault zone by whatever is the total displacement on the CFZ. There are three tracts (Fig. 4.) of outcrop of these rocks: (a) NW of the village of El Llano de Don Antonio, (b) on the south side of Rambla Cajón, (c) the tract between Cerro de Don Fernando and Playa La Manaca. Each of these tracts displays similar lithological and structural features, and all are truncated to the NW by the southern strand of the CFZ.

The section along the Granatilla river, 1 km south of the village of Sopalmo, is probably the most frequently visited section through the CFZ (Fig. 10). To the SE of the CFZ southern strand, older volcaniclastics dating from 18 Ma sit unconformably upon Burdigalian marls. The latter in turn make unconformable contact downward with heavily fractured Triassic dolomite, that passes downwards into red siltstones and sandstones. This sequence is locally tilted to the vertical, and overstepped by younger (10.5 Ma) volcaniclastics of the younger series. All of these rocks are truncated by the CFZ southern strand, which was therefore active post 10.5 Ma. On the coast a tectonic sliver of Palaeogene conglomerates, limestones and limestone breccias is interposed between the Miocene rocks and the Triassic basement rocks. This relationship is also seen at both of the outcrop tracts (a) and (b) further south-west.

The red siltstones make a tectonic contact with underlying phyllites that are generally intensely damaged and transformed into fault gouge, that must have developed prior to the CFZ faulting, but which also produces very similar fault gouge. The older, phyllite-derived gouge was probably formed in connection with the emplacement of the Alpujárride rocks onto the Nevado-Filabride basement. It is likely that the displacement of the red siltstone plus dolomite unit onto the underlying basement rocks also transported the then gently-dipping, unconformably-overlying Burdigalian marls and volcaniclastics. The older volcanic rocks and the underlying basement were tilted to the vertical prior to deposition of the younger (Serravallian/Tortonian) volcaniclastics, presumably as a result of transpression across the CFZ. At 9 Ma the large andesitic intrusion that meets the coast at Playa La Manaca was emplaced adjacent to the CFZ southern strand and, from the disposition of outcrops, inflated the anticlinal core into which it was intruded, disrupting the units in its roof. Although the SW limit of the outcrop of this intrusion does not extend into the Granatilla valley, high resolution seismic profiling (S. Nippress, pers. comm. 2010) in the valley shows that it is present at a shallow depth beneath the valley bottom. At depth, the CFZ may be intruded by substantially more andesitic intrusive sheets than are seen at the surface. At the SW of the map area the northern strand of the CFZ terminates where it runs into a wide intrusion that has localized along the fault zone.

8. Summary of the geological history of the CFZ

8.1. To the north of the CFZ

(a) Up to and including the lowermost Miocene (Aquitanian and Burdigalian), deformation and metamorphic events affected the (dominantly) pelitic and psammitic rocks of the Nevado-Filabride complex during Alpine orogenesis. Further extensional collapse with tectonic thinning led to the superposition of the lower grade rocks of the Alpujárride complex upon the Nevado-Filabride rocks. Any deposition of post-orogenic sediments or volcanic rocks up to late Serravallian has been removed by erosion or displacements on the CFZ.

(b) The first post-orogenic sediments to be preserved (U. Serravallian/L. Tortonian Saltador Fm, marine marls and sands) were deposited upon and to the north of the CFZ. These were immediately displaced and folded as the main CFZ movements took place. The CFZ was used as a conduit for the transport of magma to the surface, forming dykes and larger intrusive bodies along the fault zones, cutting the sediments of the Saltador Fm, and presumably forming minor eruptive centres along the fault zone. All eruptive material that might have been deposited north of the CFZ has now been removed by fault displacements.

(c) The U. Tortonian/L. Messinian Azagador sands then marls were deposited with unconformity, overstepping onto basement rocks to the north. They were removed by erosion as a result of transpressional uplift over the CFZ, and became tilted towards the south as the uplift of the Sierra Cabrera basement block to the north began.

(d) The Messinian sedimentary sequence was deposited unconformably above the Azagador Fm, and now forms a broadly synformal structure with the antiformal uplift over the CFZ to the south and arching over the emerging Sierra Cabrera to the north. Relatively minor strike-slip movements on the CFZ affected the Messinian and younger rocks.

(e) Assuming a minimum displacement on the CFZ of 15 km, the minimum average displacement rate on the CFZ was 2.5 mm/yr.

8.2. To the south of the CFZ

(a) Similar stacking of Alpujárride or Maláguide units upon Nevado-Filabride basement schists occurred during the L. Miocene, but with additional upper slices of non-metamorphic Palaeogene rocks being displaced upon the underlying metamorphic units.

(b) Some L. Burdigalian calc-alkaline eruptive activity occurred, leading to eroded volcanic material being incorporated within marine (U. Burdigalian) marls that sit unconformably upon horizontally layered basement rocks. During U. Burdigalian through Serravallian time, accumulation of volcaniclastic and eruptive rocks of the older volcanic series developed, followed by some lateral transport of the whole sequence on low angle faults over cataclastically deformed Alpujárride phyllites. Intense hydrothermal alteration and mineralization in the El Palaín-La Islica hydrothermal field developed.

(c) During Serravallian time, initiation of left-lateral transpressional displacements on the southern strand of the CFZ upended the older volcanics to produce a synformal flexure whose

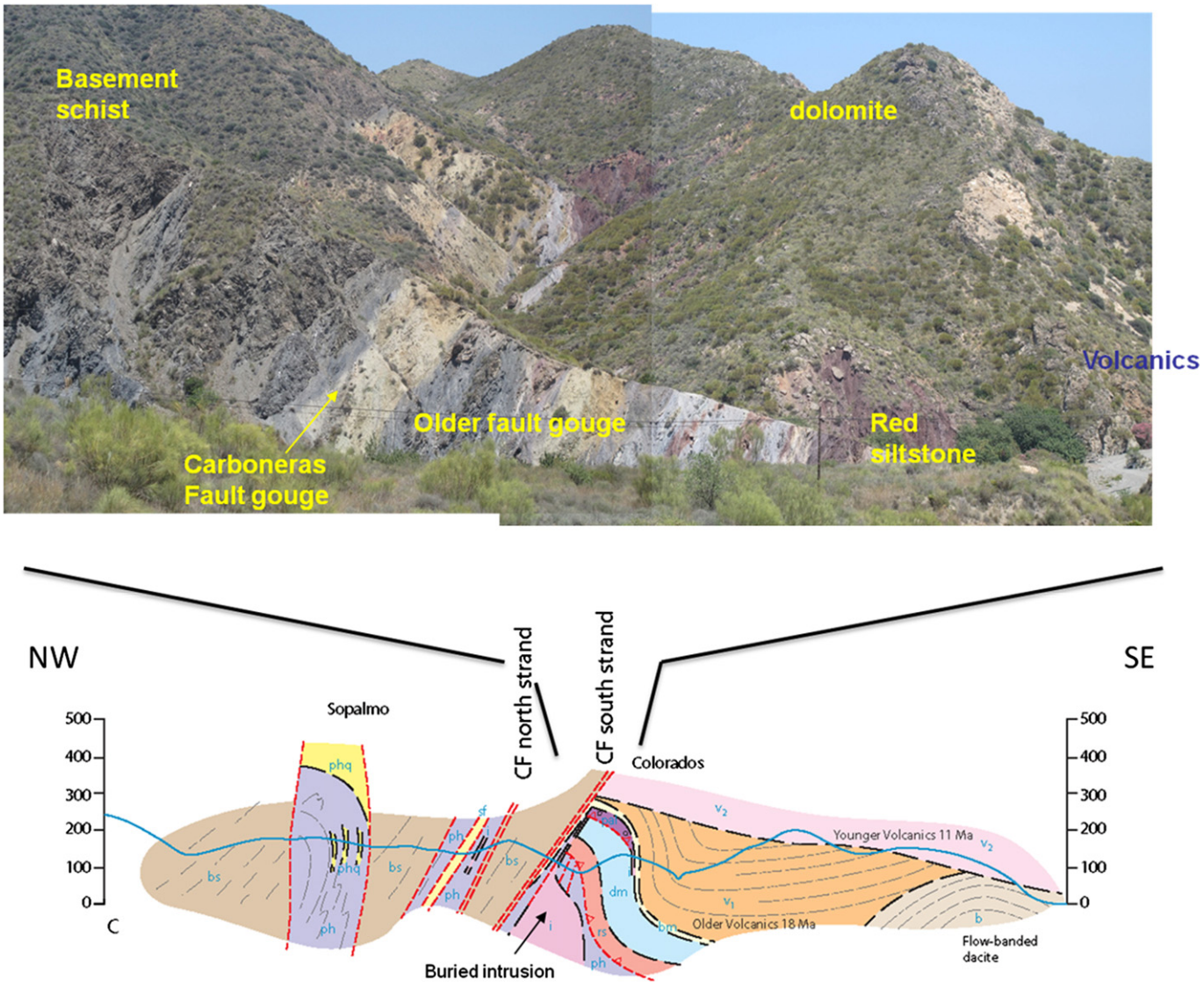

Fig. 10. Probably the most frequently visited exposure of the southern strand of the CFZ in the Granatilla river (GR 599906 4101211), looking ENE in relation to the geological cross section (D–D′ on Fig. 7). The southern strand of the Carboneras fault is the grey, 5 m wide, graphitic mica schist-derived gouge band on the left, in contact with basement schist. To the right of the gouge band is highly tectonized Burdigalian marl mixed with volcaniclastic material (yellow). Far right is a sequence of vertically-oriented volcaniclastic rocks, Burdigalian marls, Triassic dolomite (forming the prominent ridge) and a wide band of red siltstone. These units are truncated by the Carboneras fault at the top if the valley, but also tectonically overlie the wedge of older fault gouge that pre-dates and is cut by the Carboneras fault. A buried andesitic intrusion (based on shallow seismic reflection profiling and downplunge extrapolation of the intrusion exposed further N.E. on the coast) helps to form the downward widening wedge shape of the stack of units.

axis was cut by the fault to the south of the Rambla Cajón as a result of continued fault displacements.

(d) U. Serravallian and L. Tortonian time saw the beginning of deposition of the younger volcanic series, overstepping northwards onto upended basement rocks and across the fault zone. This unconformity is inferred to mark the beginning of the main movements on the CFZ. Continued movements on the CFZ removed all volcaniclastic rocks that may have been deposited to the NW of the CFZ. From Mid-Tortonian, local deposition occurred of marine carbonates (Brèche Rouge) with the volcaniclastic rocks.

(e) Deposition of the youngest volcaniclastic rocks (L. Messinian), overstepped the CFZ to the north. Continued movements on the CFZ were not large enough to displace the volcaniclastics outcropping north of the CFZ such that they were entirely removed by erosion. Messinian marine sedimentary rocks were deposited south of the CFZ, with patchy thin occurrences of the Abad marls, the evaporitic gypsum and the Feos marl. These units were progressively up-arched over the CFZ as a result of transpressional movements.

Several hundred metres of Pliocene rocks, marine then transitional to continental as uplift developed, were deposited unconformably over the whole region, both north and south of the CFZ. In the north they dip gently to the south as a result of the continued uplift of the Sierra Cabrera basement block and further south locally they arch over the CFZ as a result of continued transpression.

9. The CFZ as part of a stretching transform system

Recalling the geodynamic model for the Serravallian-Recent evolution of the Betic-Alborán region in terms of slab rollback

with the CFZ and its associated left-lateral strike-slip faults acting as a detachment zone (Fig. 2), we can propose that the fault system behaves as a stretching fault (Means, 1989), or as a velocity discontinuity in an otherwise continuous plastic flow field (Odé, 1960). The concept is illustrated in Fig. 11. The coupling of the fault system to the subducted slab means it can also be regarded as a transform fault. We do not know anything about the fault-parallel strain rate to the SE of the fault zone, but for preliminary discussion we will assume it to be zero. To the NW of the Carboneras fault system the crust is presumed to have become uniformly stretched at depth, but by discrete fault displacements in the upper crust. Stretching was parallel to the fault zone by about 50% (150 km) over 12 Ma. The fault accommodates the velocity discontinuity. At the same time the Africa-Iberia convergence continued, leading to the development of the folding that characterizes the Neogene rocks of the Carboneras area and the transpressional character of the CFZ.

As slab migration developed, the SW tip of the fault system would grow towards the SW. Thus we expect that the fault displacement history begins to develop from U. Serravallian time at its northeastern end, but that youngest activity should be seen at the south-western end. Strike-slip offset should increase progressively from zero at the NE extremity of the Alhama de Murcia fault, to a maximum of about 100 km beneath the Alborán Sea, then reduce rapidly to zero in the Rif mountains. Thus in the vicinity of Carboneras a left-lateral fault offset of about 40 km is expected provided the rocks to the SE have not been stretched. Although there is not direct field geologic evidence that the offset across the CFZ is more than 15 km, it can be noted that there is apparent offset of about 25 km between the Sierra Cabrera and Sierra Almenara (to the north-east) across the Palomares fault segment. The stretching transform model allows substantial and variable wrench displacements to develop along a fault zone whilst the relative displacements across the fault trace can decrease to zero at the fault tips, so there are no accommodation problems.

This model does not require that the stretching in the Betic-Alborán wedge remains uniform with time. It may have migrated south-west with time towards the thinner lithosphere, and in this respect there is some indication that current seismic activity, with a diffuse concentration along the left-lateral fault system, is greatest towards the north-African end of the trans-Alborán shear zone (Negredo et al., 2002; Martínez-Martínez et al., 2006).

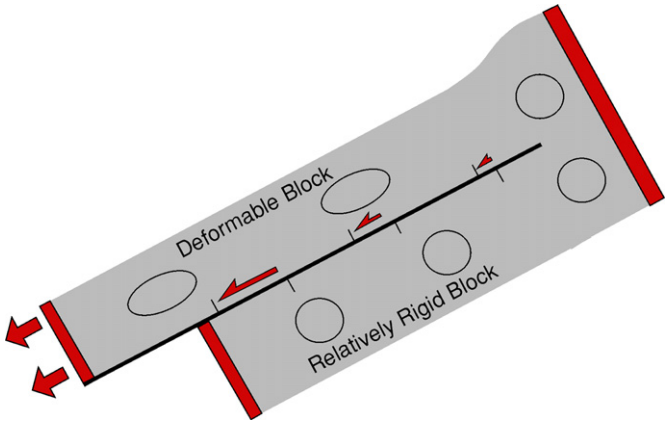

Fig. 11. Schematic illustration of a stretching fault that separates two blocks that have undergone different amounts of stretching strain parallel to the fault (after Means 1989). The fault-parallel strain in the deformed block can be homogeneous, but the displacement across the fault increases away from the tip. Accompanying shortening across the fault is not precluded. The whole system can rotate relative to an external reference frame and local shear-induced counter-clockwise rotations of embedded or overlying material in the deformed block may be expected to arise.

10. Conclusions

The structural geometry and geological history of the CFZ near Carboneras were determined through geological mapping and radiometric dating of volcaniclastic rocks that lie to the south of the CFZ and igneous rocks that intruded the fault zone coeval with its slip activity. South of the fault zone postorogenic sedimentation and calc-alkaline igneous activity began about 18 Ma BP and volcanism ended at about 6.5 Ma. All volcanic rocks are cut by fault displacements that began about 13 Ma and had largely finished by about 6 Ma.

North of the CFZ the oldest preserved postorogenic sediments date from about 11 Ma and eruptive igneous rocks are absent. Successive episodes of fault displacements and folding caused a series of four main unconformities in the sedimentary sequence to develop. Folding of the sedimentary rocks about E–W trending axes, including evidence for shortening across the CFZ and the antiformal arching of the Sierra Cabrera basement block to the north of the CFZ, is inferred to be a consequence of the continuing NW-SE convergence between Africa and Iberia. There is no direct evidence of NE–SW extension in the rocks the NW of the CFZ in the area mapped, but this is viewed as an accident of location, because low-angle extensional faults affecting upper crustal basement and cover rocks, such as are found elsewhere in the internal Betic domain, are only expected to outcrop occasionally.

The CFZ forms part of a 450 km long, segmented left-lateral strike-slip fault system interpreted to have acted as a lateral detachment or stretching transform. It separates the Betic-Alborán wedge of crustal metamorphic basement and its non-metamorphic cover rocks, extended NE-SW during upper Miocene time as a result of subducted slab rollback, from less or differently deformed rocks to the SE. This model suggests 40 km of lateral offset has accumulated in the vicinity of Carboneras, although there is direct geological evidence for only about 15 km of this.

We infer that slab rollback started with the onset of CFZ displacements (13 Ma), rather later than inferred by Lonergan and White (1997), and extending over a lesser distance, but slightly earlier than inferred by Gutscher (2012). The main phase of movement developed through the U. Serravallian and Tortonian stages (12–7 Ma) with calc-alkaline igneous activity, including intrusions into the developing fault zone. From the lower Messinian stage onward volcanic activity ceased and only minor strike-slip displacement activity is recorded, probably implying that the main rollback displacements had been completed by the end of the Miocene period. From the middle part of the Messinian stage (6 Ma through present) emergence and uplift are dominant effects in the Carboneras region, together with continued NW–SE shortening, including the antiformal uplifts of the basement blocks (e.g. Sierras Cabrera, Alhamilla, Los Filabres).

Acknowledgements

This work was carried out with support from UK NERC, grant NE/F019475/1, and in part whilst EHR was supported as a visiting scientist at the Institute of Earth Sciences 'Jaume Almera' (CSIC), Barcelona, by the Spanish Ministry of Education and Sciences. Fellow members of the research group and those who provided support during fieldwork are: Andreas Rietbrock, Stuart Nippress, Rochelle Taylor, Oshaine Blake, John Gates, Joe Tant, Lindy Walsh and Antonio Ruiz-Zamora. Anne Mather and an anonymous referee provided comments that helped in producing the final manuscript.

The Consejería del Medio-Ambiente, Junta de Andalucía gave permissions for geological work to be carried out in the Gabo de Gata-Nijar Natural Park area.

Drafting of main map and sections by Richard Hartley.

Appendix A. Supporting material

Supplementary data related to this article can be found online at doi:10.1016/j.jsg.2012.08.009.

References

Bell, J.W., Amelung, F., King, G.C.P., 1997. Preliminary late quaternary slip history of the Carboneras fault, southeastern Spain. Geodynamics 24, 5–14.

Ben Zion, Y., Shi, Z., 2005. Dynamic rupture on a material interface with spontaneous generation of plastic strain in the bulk. Earth and Planetary Science Letters 236, 486–496.

Billi, A., Di Toro, G., 2008. Fault-related carbonate rocks and earthquake indicators: recent advances and future trends. In: Landowe, S.J., Hammler, G.M. (Eds.), Structural Geology: New Research. Nova Science Publishers, Inc., New York, ISBN 978-1-60456-827-1, pp. 1–24.

Boorsma, L.J., 1992. Syn-tectonic sedimentation in a Neogene strike-slip basin containing a stacked Gilbert-type delta (S. E. Spain). Sedimentary Geology 81, 105–123.

Booth-Rea, G., Azañón, J.M., Martínez-Martínez, J.M., Vidal, O., García-Dueñas, V., 2003. Análisis estructural y evolución tectonometamórfica del basamento de las cuencas Neógenas de Vera y Huercal-Overa, Béticas Orientales. Reviews Geological Society España 16, 193–211.

Booth-Rea, G., Azañón, J.M., Azor, A., García-Dueñas, V., 2004. Influence of strike-slip fault segmentation on drainage evolution and topography. A case study: the Palomares Fault Zone (southeastern Betics, Spain). Journal of Structural Geology 26, 1615–1632.

Braga, J.C., Martín, J.M., Riding, R., Aguirr, J., Sánchez-Almazo, I.M., Dinarès-Turell, 2006. Testing models for the Messinian salinity crisis: the Messinian record in Almería, SE Spain. Journal of Sedimentary Geology 188–189, 131–154.

Calvo, M., Osete, M.L., Vegas, R., 1994. Paleomagnetic rotations in opposite senses in southeastern Spain. Geophysical Research Letters 21, 761–764.

Carrillo Rosúa, F.J., Morales Ruano, S., Fenoll Hach-alí, P., 2002. The three generations of gold in the Palai–Islica epithermal deposit, southeastern Spain. The Canadian Mineralogist 40, 1465–1481.

Chalouan, A., Michard, A., 2004. The Alpine Rif Belt (Morocco): a case of mountain building in a subduction-subduction-transform fault triple junction. Pure and Applied Geophysics 161, 489–519. http://dx.doi.org/10.1007/s00024-003-2460-7.

De Larouzière, F.D., Bolze, J.I.P., Bordet, I.P., Hernandez, J.C., Montenat, C., Ott d'Estevou, P., 1988. The Betic segment of the lithospheric trans-Alborán shear zone during the Late Miocene. Tectonophysics 152, 41–52.

Diaz, J., Gallart, J., Villaseñor, A., Mancilla, F., Pazos, A., Córdoba, D., Pulgar, J.A., Ibarra, P., Harnafi, M., 2010. Mantle dynamics beneath the Gibraltar Arc (western Mediterranean) from shear-wave splitting measurements on a dense seismic array. Geophysical Research Letters 37, L18304. http://dx.doi.org/10.1029/2010GL044201.

Faccenna, C., Piromallo, C., Crespo-Blanc, A., Jolivet, L., Rossetti, F., 2004. Lateral slab deformation and the origin of the western Mediterranean arcs. Tectonics 23, TC1012. http://dx.doi.org/10.1029/2002TC001488.

Faulkner, D.R., Rutter, E.H., 2000. Comparisons of water and gas permeability in natural clay-bearing fault gouge under high pressure at 20 degrees C. Journal of Geophysical Research 105, 16415–16426.

Faulkner, D.R., Rutter, E.H., 2003. Effect of temperature and non-hydrostatic stress on the permeability of clay-bearing fault gouge. Journal of Geophysical Research 108 (B5), 2227. http://dx.doi.org/10.1029/2001JB001581.

Faulkner, D.R., Lewis, A.C., Rutter, E.H., 2003. On the internal structure and mechanics of large strike-slip fault zones: field observations of the Carboneras fault zone, S.E. Spain. Tectonophysics 367, 235–251.

Fortuin, A.R., Krijgsman, W., 2003. The Messinian of the Nijar Basin (SE Spain): sedimentation, depositional environments and paleogeographic evolution. Sedimentary Geology 160, 213–242.

Garcia Monzón, G., Kampschuur, W., Verburg, J., 1974. Mapa Geologico de España, sheet 1031, scale 1:50000, (Sorbas). Instituto Geologico y Minero de España, Madrid.

García-Dueñas, V., Balanyá, J.C., Martínez-Martínez, J.M., 1992. Miocene extensional detachments in the outcropping basement of the northern Alborán basin (Betics) and their tectonic implications. Geo-Marine Letters 12, 88–95.

Giaconia, F., Booth-Rea, G., Martínez-Martínez, J.M., Azañón, J.M., 2011. Extensional transfer faults versus transcurrent faults in the eastern Betics, an example from the Sorbas basin (SE Spain). Geophysical Research Abstracts 13. EGU2011-4011-1.

Grácia, E., Pallás, R., Soto, J.-I., Comas, M., Moreno, X., Masana, E., Santanach, P., Diez, S., García, M., Doñobeitia, J., 2006. Active faulting offshore SE Spain (Alborán Sea): Implications for earthquake hazard assessment in the Southern Iberian Margin. Earth and Planetary Science Letters 241, 734–749.

Gutscher, M.A., 2012. Subduction beneath Gibraltar? Recent studies provide answers. EOS 93, 133–134.

Gutscher, M.A., Malod, J., Rehault, J.P., Contrucci, I., Klingelhoefer, F., Mendes-Victor, L., Spakman, W., 2002. Evidence for active subduction beneath Gibraltar. Geology 30, 1071–1074.

Huibregtse, P., van Alebeek, H., Zaal, M., Biermann, C., 1998. Palaeostress analysis of the northern Nijar and southern Vera basins: constraints for the Neogene displacement history of major strike-slip faults in the Betic Cordilleras, S.E. Spain. Tectonophysics 300, 79–101.

Jourdan, F., Verati, C., Féraud, G., 2007. Intercalibration of the Hb3gr $^{40}Ar/^{39}Ar$ dating standard. Chemical Geology 231, 177–189.

Kampschuur, W., Rondeel, H.E., 1975. The origin of the Betic Orogen, southern Spain. Tectonophysics 7, 39–56.

Keller, J.V.A., Hall, S.H., Dart, C.J., McClay, K.R., 1995. The geometry and evolution of a transpressional strike-slip system: the Carboneras Fault, SE Spain. Journal of the Geological Society 152, 339–351. http://dx.doi.org/10.1144/gsjgs.152.2.0339.

Krijgsman, W., Fortuin, A.R., Hilgen, F.J., Sierro, F.J., 2001. Astrochronology for the Messinian Sorbas basin (SE Spain) and orbital (precessional) forcing for evaporite cyclicity. Sedimentary Geology 140, 43–60.

LeBlanc, D., Olivier, P., 1984. Role of strike-slip faults in the Betic-Rifian orogeny. Tectonophysics 101, 345–355.

Lonergan, L., 1993. Timing and kinematics of deformation in the Maláguide complex, internal zone of the Betic Cordillera, southeast Spain. Tectonics 12, 460–476.

Lonergan, L., Platt, J.P., 1995. The Maláguide-Alpujárride boundary: a major extensional contact in the Internal Zone of the eastern Betic Cordillera, S. E. Spain Journal of Structural Geology 17, 1655–1671.

Lonergan, L., White, N., 1997. Origin of the Betic-Rif mountain belt. Tectonics 16, 504–522.

Ludwig, K., 2003. Isoplot/Ex, Version 3: a Geochronological Toolkit for Microsoft Excel. Geochronology Center, Berkeley, USA.

Maher, E., Harvey, A.M., 2008. Fluvial system response to tectonically induced base-level change during the Late-Quaternary: the Rio Alias southeast Spain. Geomorphology 100, 180–192.

The Messinian record of the outcropping marginal Alborán Basin deposits: significance and implications. In: Martín, J.M., Braga, J.C., Sánchez-Almazo, I., Zahn, R., Comas, M.C., Klaus, A. (Eds.), Proceedings of the Ocean Drilling Program, Scientific Results, pp. 161–543.

Martin, J.M., Braga, J.C., Betzler, C., 2003. Late Neogene-recent uplift of the Cabo de Gata volcanic province, Almeria, SE Spain. Geomorphology 50, 27–42.

Martínez-Martínez, J.M., Booth-Rea, G., Azañón, J.M., Torcal, F., 2006. Active transfer fault zone linking a segmented extensional system (Betics, southern Spain): Insight into heterogeneous extension driven by edge delamination. Tectonophysics 422, 159–173.

Mather, A.E., Braga, J.C., Martin, J.M., Harvey, A.M., 2001. Introduction to the Neogene geology of the Sorbas basin. In: Mather, A.E., Martin, J.M., Harvey, A.M., Braga, J.C. (Eds.), A Field Guide to the Neogene Sedimentary Basins of the Almería Province, S. E. Spain. Blackwell, Oxford, pp. 9–28.

Means, W.D., 1989. Stretching faults. Geology 17, 893–896. http://dx.doi.org/10.1130/0091-7613(1989)017<0893:SF>2.3.CO;2.

Meijninger, B.M.L., Vissers, R.L.M., 2006. Miocene extensional basin development in the Betic Cordillera, SE Spain revealed through analysis of the Alhama de Murcia and Crevillente Faults. Basin Research 18, 547–571. http://dx.doi.org/10.1111/j.1365-2117.2006.00308.x.

Mitchell, T.M., Ben-Zion, Y., Shimamoto, T., 2011. Pulverized fault rocks and damage asymmetry along the Arima-Takatsuki tectonic line, Japan. Earth and Planetary Science Letters 308, 284–297.

Monie, P., Galindo-Zaldivar, J., Gonzalez Lodeiro, F., Goffe, B., Jabaloy, A., 1991. $^{40}Ar/^{39}Ar$ geochronology of Alpine tectonism in the Betic Cordilleras (southern Spain). Journal of the Geological Society, London 148, 289–297.

Morales Ruano, S., Carrillo Rosúa, F.J., Hach-alí, P.F., de la Fuente Chacón, F., Contreras López, E., 2000. Epithermal cu–au mineralization in the Palai–Islica deposit, Almería, southeastern Spain: fluid-inclusion evidence for mixing of fluids as a guide to gold mineralization. The Canadian Mineralogist 38, 553–565.

Negredo, A.M., Bird, P., Sanz de Galdeano, C., Buforn, E., 2002. Neotectonic modeling of the Ibero-Maghrebian region. Journal of Geophysical Research 107, 2292. http://dx.doi.org/10.1029/2001JB000743.

Odé, H., 1960. Faulting as a velocity discontinuity in plastic deformation. In: Griggs, D., Handin, J. (Eds.), Rock Deformation. Geological Society of America Memoir, vol. 79. Waverly Press, Baltimore, pp. 293–321.

Platt, J.P., Vissers, R.L.M., 1989. Extensional collapse of thickened continental lithosphere: a working hypothesis for the Alborán sea and Gibraltar arc. Geology 17, 540–543.

Platt, J.P., Whitehouse, M.J., 1999. Early Miocene high-temperature metamorphism and rapid exhumation in the Betic Cordillera (Spain): evidence from U–Pb zircon ages. Earth and Planetary Science Letters 171, 591–605.

Platt, J., Allerton, S., Kicker, A., Platzman, E., 1995. Origin of the western subbetics (southern Spain): palaeomagnetic and structural evidence. Journal of Structural Geology 17, 765–775.

Platt, J.P., Kelley, S.P., Carter, A., Orozco, M., 2005. Timing of tectonic events in the Alpujárride complex, Betic Cordillera, southern Spain. Journal of the Geological Society 162, 451–462.

Platzman, E., 1992. Paleomagnetic rotations and the kinematics of the Gibraltar arc. Geology 20, 311–314.

Reicherter, K.R., Reiss, S., 2001. The Carboneras Fault Zone (southeastern Spain) revisited with ground penetrating radar – quaternary structural styles from high-resolution images. Netherlands Journal of Geosciences/Geologie en Mijnbouw 80, 129–138.
Rutter, E.H., 1983. Pressure solution in nature, theory and experiment. Journal of the Geological Society 140, 725–740.
Rutter, E.H., White, S.H., 1979. The microstructure and rheology of fault gouges produced experimentally at temperatures up to 400 °C. Bulletin Minéralogie 102, 101–109.
Rutter, E.H., Maddock, R.H., Hall, S.H., White, S.H., 1986. Comparative microstructures of naturally and experimentally produced clay-bearing fault gouge. Pure and Applied Geophysics 124, 3–30.
Sanz de Galdeano, C., 1990. Geologic evolution of the Betic Cordilleras in the Western Mediterranean, Miocene to the present. Tectonophysics 172, 107–119.
Sanz de Galdeano, C., Alfaro, P., 2004. Tectonic significance of the present relief of the Betic Cordillera. Geomorphology 63, 175–190.
Sanz de Galdeano, C., Buforn, E., 2005. From strike-slip to reverse reactivation: the Crevillente Fault System and seismicity in the Bullas-Mula area (Betic Cordillera, SE Spain). Geologica Acta 3, 241–250.
Scotney, P., Burgess, R., Rutter, E.H., 2000. ^{40}Ar-^{39}Ar dating of the Cabo de Gata volcanic series and displacements on the Carboneras fault, S.E. Spain. Journal of the Geological Society 157, 1003–1008.
Serrano, F., 1990a. Presencia de Serravallianse marino en la Cuenca de Níjar (Cordillera Bética, Espana). Geoaceta 7, 95–97.
Serrano, F., 1990b. El Mioceno Medio en el area de Nijar (Almeria, España). Reviews Geological Society España 3, 65–77.
Serrano, F., Gonzáles Donoso, J.M., 1989. Cronoestratigrafía de la sucesión volcanosedimentaria del área de Carboneras (Sierra de Gata, Almería). Reviews Geological Society España 2, 143–151.
Sierro, F.J., Hilgen, J., Krijgsman, J.W., Flores, J.A., 2001. The Abad composite (SE Spain): a Messinian reference section for the Mediterranean and the APTS. Palaeogeography, Palaeoclimatology, Palaeoecology 168, 141–169.
Solum, J.G., van der Pluijm, B.A., 2009. Quantification of fabrics in clay gouge from the Carboneras fault, Spain and implications for fault behaviour. Tectonophysics 475, 554–562.
Stapel, G., Moeys, R., Biermann, C., 1996. Neogene evolution of the Sorbas basin (SE Spain) determined by paleostress analysis. Tectonophysics 255, 291–305.
Torres-Roldán, R., 1979. The tectonic subdivision of the Betic Zone, Betic Cordilleras, Southern Spain): Its significance and one possible geotectonics scenario of the westernmost Alpine belt. American Journal of Science 279, 19–51.
Turner, S.P., Platt, J.P., George1, R.M.M., Kelley, S.P., Pearson, D.G., Nowell, G.M., 1999. Magmatism associated with orogenic collapse of the Betic–Alboran domain, SE Spain. Journal of Petrology 40, 1011–1036.
Uwe, M.R., Krautworst, T., Brachert, C., 2003. Sedimentary facies during early stages of flooding in an extensional basin: the Brèche Rouge de Carboneras (Late Miocene, Almería, S. E. Spain). International Journal of Earth Sciences (Geol. Rundsch.) 92, 610–623. http://dx.doi.org/10.1007/s00531-003-0337-8.
Van der Poel, H.M., 1992. Foraminiferal biostratigraphy and palaeoenvironments of the Miocene-Pliocene Carboneras-Nijar basin (S.E. Spain). Scripta Geologica 102, 1–31.
Vissers, R.L.M., 2012. Extension in a convergent tectonic setting: a lithospheric view on the Alboran system of SW Europe. Geologica Belgica 15, 53–72.
Völk, H.R., Rondeel, H.E., 1964. Zur gliederung des Jungtertiars im Becken von Vera, Südost Spanien. Geologie en Mijnbouw 43, 310–315.
Westra, G., 1969. Petrogenesis of a Composite Metamorphic Facies Series in an Intricate Fault-zone in the South-eastern Sierra Cabrera, S.E. Spain. GUA Series in Geology, Geological Institute, University of Amsterdam, 166 pp.
Zeck, H.P., 1996. Betic-Rif orogeny: subduction of Mesozoic Tethys lithosphere under eastward drifting Iberia, slab detachment before 22 Ma, and subsequent uplift and extensional tectonics. Tectonophysics 254, 1–16.
Zeck, H.P., 2004. Rapid exhumation in the Alpine belt of the Betic-Rif (W Mediterranean): tectonic Extrusion. Pure and Applied Geophysics 161, 477–487. http://dx.doi.org/10.1007/s00024-003-2459-0.